Publié par :
Published by:
Publicación de la:

Faculté des sciences de l'administration
2325, rue de la Terrasse
Pavillon Palasis-Prince, Université Laval
Québec (Québec) Canada G1V 0A6
Tél. Ph. Tel. : (418) 656-3644
Télec. Fax : (418) 656-7047

Disponible sur Internet :
Available on Internet
Disponible por Internet :

http://www4.fsa.ulaval.ca/la-recherche/publications/documents-de-travail/

DOCUMENT DE TRAVAIL 2018-017

Strategic and Operational Decision-Making in Expanding LNG Supply Chains

Rogier DELUSTER
Paul BUIJS
Leandro C. COELHO
Evrim URSAVAS

Document de travail également publié par le Centre interuniversitaire de recherche sur les réseaux d'entreprise, la logistique et le transport, sous le numéro CIRRELT-2018-35

Août 2018

Dépôt legal – Bibliothèque et Archives nationales du Québec, 2018
Bibliothèque et Archives Canada, 2018

ISBN 978-2-89524-474-5 (PDF)

Strategic and Operational Decision-Making in Expanding LNG Supply Chains

Rogier Deluster[1], **Paul Buijs**[1*], **Leandro C. Coelho**[1,2], **Evrim Ursavas**[1]

[1] Department of Operations, Faculty of Economics and Business, University of Groningen, The Netherlands
[2] Interuniversity Research Centre on Enterprise Networks, Logistics and Transportation (CIRRELT) and Department of Operations and Decision Systems, 2325, rue de la Terrasse, Université Laval, Québec, Canada, G1V 0A6

**Corresponding author: p.buijs@rug.nl*

ABSTRACT

The European Union aims for a 20% reduction in greenhouse gas emissions by 2020, compared to 1990 levels, and recognizes the transition to liquefied natural gas (LNG) as a sustainable fuel in the shipping and road transport industry as an opportunity to reach those goals. The lack of a mature LNG fueling infrastructure requires establishing new (satellite) terminals on-shore and bunker barges and tanker trucks to distribute LNG, all of which are extremely expensive. The network design problem to further develop the current supply chain for LNG as a fuel can be defined as a Two-Echelon Capacitated Location Routing Problem with Split Deliveries (2E-CLRPSP). An important feature of this specific problem is that direct deliveries are allowed from (satellite) terminals, which makes the problem much harder to solve than the existing location routing literature suggests. In this paper, we improve the performance of a hybrid exact algorithm. We apply our algorithm to a real-life network design problem for the LNG supply chain in the Netherlands, as well with its expansion into Europe. We show that the use of satellite terminals, supporting the large-scale LNG terminal in the Port of Rotterdam, is highly dependent on the capacity of the satellite and the fees that need to be paid at the large-scale terminal when loading LNG.

Keywords: Sustainability, alternative fuel, liquefied natural gas (LNG), network design problem, neighborhood search, exact algorithm.

Acknowledgments: This work was supported by the Natural Sciences and Engineering Research Council of Canada (NSERC) under grant 2014-05764, and by the INTEREG V A project LNG PILOTS. We thank Calcul Québec for providing high performance computing facilities. These supports are gratefully acknowledged.

1 Introduction

Liquefied natural gas (LNG) is becoming increasingly popular as an alternative fuel for road-freight and maritime transportation. LNG is natural gas that is converted to a liquid state by cooling it down to approximately $-162\,^{\circ}\mathrm{C}$. In this liquid state it takes up much less volume compared to a (compressed) gaseous state, which makes LNG particularly suitable as a fuel for long-haul trucking and shipping. Using LNG as a transportation fuel is a recent development, and the supply chain through which the fuel is made available to its end users is still noticeably in development Thunnissen et al. [2016], Post et al. [2017]. This so-called small-scale LNG supply chain extends the large-scale supply chain that facilitates global trade in LNG.

Developing the small-scale LNG supply chain involves large investments in facilities, vehicles and equipment to distribute the fuel. In the last few years, many LNG fuel stations have been opened and several ports can now supply ships with LNG as a fuel. The LNG is supplied from large import terminals, where specialized tanker trucks and bunker barges can load LNG to be transported to fuel stations and ports. Since there are only a few, very large import terminals around the world, new (satellite) terminals may need to be opened to efficiently transport LNG to ports and fuel stations in areas located further from the import terminals. Deciding whether to open one or more (satellite) terminals, and if so, to determine their locations and sizes, are critically important decisions in the development of small-scale LNG supply chains, and may have a profound impact on the routing decisions of the tanker trucks and bunker barges.

This paper presents a new problem aimed at finding an efficient and cost-effective network design for fulfilling two types of demand for LNG as a fuel: road demand (i.e., fuel stations for trucks) and waterway demand (i.e., ports where ships take on LNG). Demand is assumed to be deterministic. The network can consist of two types of facilities: a first level, consisting of large import terminals; and a second level, consisting of smaller-sized satellite terminals. Opening a facility is associated with fixed costs, and if opened, there are operating costs per unit volume of LNG. The facilities have a given capacity that can be upgraded at an additional cost. Using tanker trucks and bunker barges as mode of transportation, the LNG can be transported from an import terminal to the fuel stations and ports directly, or via a satellite. Each of these vehicle types has a given capacity and is associated with a certain fixed and variable cost. The problem is to open and/or upgrade facilities at the first and second level of the network, to decide upon the routes of the tanker trucks and bunker barges, and to allocate inventories, while minimizing facility and transportation costs over multiple time periods.

The problem we study consists of attributes that have not been considered in combination in previous studies. We hereby present the related literature. The concept of determining location and routing decisions simultaneously was put forward by Boventer [1961], Maranzana [1964] and Watson-Gandy and Dohrn [1973] which led to the research field known as the location-routing problem (LRP). Surveys on this topic are published by Min et al. [1998], Nagy and Salhi [2007], Balakrishnan et al. [1987], Prodhon and Prins [2014] and Drexl and Schneider [2015]. In the past decades, numerous extensions to the

LRP have been identified. Karaoglan et al. [2012], for example, worked on the LRP with simultaneous pickup and delivery by means of a branch-and-cut algorithm. Prins et al. [2007] considered capacitated routes and depots in the LRP structure. Several authors studied the multi-period setting since variations in the demand patterns or regulations over time may considerably change the design of the distribution network. Prodhon [2011] uses visiting patterns to customers and assigns customers to facilities for each period. A customer can be visited from different depots over time. Albareda-Sambola et al. [2012] worked on the dynamic LRP and by considering different scales within the time horizon reflected on the stability of location decisions as compared to routing decisions.

To solve the variety of LRPs different techniques based on heuristic methods and exact algorithms have been developed Albareda-Sambola et al. [2005], Escobar et al. [2014], Hof et al. [2017], Koç et al. [2016], Laporte et al. [1988], Menezes et al. [2016]. Contardo et al. [2013] developed an exact technique based on cut and column generation. They introduced new set of inequalities and tested instances from Perl and Daskin [1985], Tuzun and Burke [1999], Barreto [2004], Prins et al. [2006], Akca et al. [2008] and Baldacci et al. [2011] and improved the bounds found in the literature. In a recent work Schneider and Löffler [2017] developed a tree-based search heuristic that uses a large composite neighborhood.

An important attribute when studying the LRPs is the hierarchical structure of the network and the existence of intermediate facilities Santos et al. [2015]. Considering this, Guastaroba et al. [2016] provided a survey on transportation problems where the existence of intermediate facilities has significant influence on cost and distribution structure. A survey of two-echelon LRPs has been published by Cuda et al. [2015]. Rieck et al. [2014] studied a LRP where pickup and deliveries are performed on local multi-stop routes, starting and ending at an intermediate facility. They considered a static problem where one aggregate, representative planning period is assumed.

In this paper, we study a variant of the LRP which can be defined as a Two-Echelon Capacitated Location Routing Problem with Split Deliveries (2E-CLRPSP). We further extend this problem with direct deliveries, and to tackle its complexity we propose three enhancements on an existing hybrid exact algorithm combining branch-and-bound and several local search structures. We apply our algorithm to find solutions for the small-scale LNG supply chain in Europe and gain interesting insights in this real-life network design problem.

2 Formal description and mathematical formulation

In this network design problem for the LNG distribution, the commodity is consumed by ships at ports along waterways, or by cars at fuel stations along roads. Let $\mathcal{C}$ be the set of all demand points consisting of waterway locations $\mathcal{C}_w$ and road locations $\mathcal{C}_r$. The network consists of roadway edges $\mathcal{E}_r$ and waterway edges $\mathcal{E}_w$. All ports can be reached through road and waterways; however, the LNG gas stations can only be reached through roadways. The set $\mathcal{K}$ indicates the type of vehicles available. Demand can be satisfied by replenishing fuel stations and ports via tanker trucks and bunker barges, jointly referred

to as vehicles. We call the set of vehicles $\mathcal{M}_k$ ($k = 1$ for bunker barges, 2 for tanker trucks).

The set $\mathcal{D}$ contains the locations of import terminals, while $\mathcal{S}$ defines the set of locations of all possible satellite facilities to be installed. Satellites are modeled as two nodes, one for the inbound deliveries in which satellites are regarded as customers, under the set $\mathcal{S}_c$, and an outbound side represented by set $\mathcal{S}_d$ in which satellites are regarded as a depot capable of providing the commodity to both types of vehicles. The capacity of satellite facilities can be expanded by investing in new modular storage tanks. For each facility type $\mathcal{F}$, there is a predefined module size available based on their initial capacities.

The problem is then defined on an undirected graph $\mathcal{G} = (\mathcal{V}, \mathcal{E})$, where $\mathcal{V} = \mathcal{D} \cup \mathcal{S} \cup \mathcal{C}$ and $\mathcal{E} = \mathcal{E}_r \cup \mathcal{E}_w$. Terminals and satellites have an initial construction cost F_i^e for facility type $e \in \mathcal{F}$ and location $i \in \mathcal{D} \cup \mathcal{S}$, operating cost O_i^e and upgrade costs U_i^e. The initial capacity of facility e located at i is B_i^e. Vehicles have a fixed usage cost W^k for $k \in \mathcal{K}$, acquisition cost H^k, and a variable cost V^k per kilometer. The problem is defined over a planning horizon $\mathcal{T}$ and the demand of node i is known for every period t and denoted D_i^t.

The variables used to model the problem are as follows. Let α_{ijd}^{vkt} be a binary variable indicating whether vehicle v of type k starting its trip from terminal d travels edge $(i, j) \in \mathcal{E}$ in period t, and β_{ijs}^{vt} be a binary variable if vehicle v starting its trip at satellite s travels edge $(i, j) \in \mathcal{E}_r$ in period t. Note that satellites can only be the start of the trip for tanker trucks, hence the type of the vehicle is not embedded into the variable β, and that only the road network is used when considering edge (i, j). When a satellite is visited by a bunker barge, this one had started its trip at a terminal. Location decisions are modeled using binary variables γ_i^{et} equal to 1 if facility type e is located at node i in period t. In that case, ι_i^{et} indicates the capacity of facility type e installed at location i in period t, and ζ_i^{et} the number of upgrade modules installed at facility e at location i in period t.

Delivery variables δ_{dj}^{vkt} indicate the number of m^3 of LNG delivered to customer $j \in \mathcal{C}$ from terminal d using vehicle v of type k in period t. Likewise, ϵ_{sj}^{vt} indicates the volume of LNG delivered to customer $j \in \mathcal{C}$ from satellite $s \in \mathcal{S}_d$ using vehicle v in period t. Fleet size and mix decisions are modeled using variables η^{ekt} to indicate the number of new vehicles of type k in facility e in period t, while κ^{ekt} measures the size of the fleet of vehicle type k at facility e in period t. Finally, inventory is controlled using variables θ_i^t to measure the volume available at satellite $i \in \mathcal{S}_d$ in period t.

The problem can then be formulated as follows.

$$
\begin{aligned}
&\text{minimize} \sum_{i \in \mathcal{D} \cup \mathcal{S}_d} \sum_{e \in \mathcal{F}} \left(\gamma_i^{eT} F_i^e + \zeta_i^{eT} U_i^e + \sum_{t \in \mathcal{T}} \iota_i^{et} O_i^e \right) + \\
&\sum_{t \in \mathcal{T}} \left(\sum_{j \in \mathcal{N}} \left(\sum_{k \in \mathcal{K}} \sum_{d \in \mathcal{D}} \sum_{v \in \mathcal{M}_k} \alpha_{djd}^{vkt} W_k + \sum_{s \in \mathcal{S}_d} \sum_{w \in \mathcal{M}_2} \beta_{sjs}^{wt} W_2 \right) + \sum_{e \in \mathcal{F}} \sum_{k \in \mathcal{K}} \eta^{ekt} H_k \right) + \\
&\sum_{t \in \mathcal{T}} \sum_{i \in \mathcal{N}} \sum_{j \in \mathcal{N}} \left(\sum_{k \in \mathcal{K}} \sum_{d \in \mathcal{D}} \sum_{v \in \mathcal{M}_k} \alpha_{ijd}^{vkt} L_{ij}^k V_k + \sum_{s \in \mathcal{S}_d} \sum_{w \in \mathcal{M}_2} \beta_{ijs}^{wt} L_{ij}^2 V_2 \right) \qquad (1)
\end{aligned}
$$

Set	*Description*
$\mathcal{V}$	Nodes
$\mathcal{E}$	Edges
$\mathcal{E}_w$	Waterway edges
$\mathcal{E}_r$	Roadway edges
$\mathcal{D}$	Candidate terminal locations
$\mathcal{S}$	Candidate satellite locations
$\mathcal{S}_d$	Satellite locations acting as a depot
$\mathcal{S}_c$	Satellite locations acting as a customer
$\mathcal{F}$	Facility types
$\mathcal{C}$	Customers
$\mathcal{C}_w$	LNG water demand points
$\mathcal{C}_r$	LNG road demand points
$\mathcal{K}$	Vehicle types
$\mathcal{M}_k$	All vehicles (tanker trucks and bunker barges)
$\mathcal{T}$	Periods
Parameter	*Description*
F_i^e	Opening cost of facility type $e \in \mathcal{F}$ at location $i \in \mathcal{D} \cup \mathcal{S}$
O_i^e	Operating cost of facility type $e \in \mathcal{F}$ at location $i \in \mathcal{D} \cup \mathcal{S}$ per m^3
U_i^e	Upgrade cost of facility type $e \in \mathcal{F}$ at location $i \in \mathcal{D} \cup \mathcal{S}$
B_i^e	Initial capacity of facility type $e \in \mathcal{F}$ at location $i \in \mathcal{D} \cup \mathcal{S}$
C^e	Capacity of a module for upgrading or downgrading facility type $e \in \mathcal{F}$
A^e	Maximum capacity of facility type $e \in \mathcal{F}$
H^k	Cost of a new vehicle of type $k \in \mathcal{K}$
V^k	Variable cost of vehicle type $k \in \mathcal{K}$ per km
W^k	Fixed cost of using a vehicle of type $k \in \mathcal{K}$
G^k	Capacity of vehicle type $k \in \mathcal{K}$
E^k	Minimum quantity delivered using vehicle k
I^{ek}	Initial fleet size of vehicle type $k \in \mathcal{K}$ at facility type $e \in \mathcal{F}$
R^{ek}	Maximum number of vehicles of type $k \in \mathcal{K}$ at facility type $e \in \mathcal{F}$
D_i^t	Demand at location $i \in \mathcal{C}$ in period $t \in \mathcal{T}$
L_{ij}^k	Distance between locations i and j for vehicle type $k \in \mathcal{K}$
Variable	*Description*
α_{ijd}^{vkt}	if vehicle v of type k starting from terminal d travels edge $(i,j) \in \mathcal{E}$ in period t
β_{ijs}^{vt}	if vehicle v (of type tanker truck) starting from satellite s travels edge $(i,j) \in \mathcal{E}_r$ in period t
γ_i^{et}	if facility type e is opened at location i in period t
δ_{dj}^{vkt}	volume delivered to j from to terminal d using vehicle v of type k in period t
ϵ_{sj}^{vt}	volume delivered to j from satellite s using vehicle v in period t
ζ_i^{et}	number of module upgrades at facility i in period t
η^{ekt}	number of new vehicles of type k added to facility e in period t
θ_i^t	inventory at satellite i in period t
ι_i^{et}	capacity of facility type e at location i in period t
κ^{ekt}	fleet size of vehicle type k at facility e in period t

The objective function is formulated in (1) and minimizes the facilities' construction, upgrade and periodic operating costs in the first part. Similarly, vehicles' fixed and upgrade costs are minimized in the second part. The third part entails the variable routing costs. The constraints of the model are as follows:

$$\gamma_i^{1t} = 0 \qquad i \in \mathcal{N} \setminus \mathcal{D}, t \in \mathcal{T} \qquad (2)$$

$$\gamma_i^{2t} = 0 \qquad i \in \mathcal{N} \setminus \mathcal{S}, t \in \mathcal{T} \qquad (3)$$

$$\gamma_i^{1t} + \gamma_i^{2t} \leq 1 \qquad i \in \mathcal{D} \cup \mathcal{S} \qquad (4)$$

$$\gamma_i^{et} \geq \gamma_i^{e,t-1} \qquad i \in \mathcal{D} \cup \mathcal{S}, e \in \mathcal{F}, t \in \mathcal{T} \qquad (5)$$

$$\gamma_i^{2t} = \gamma_j^{2t} \qquad i \in \mathcal{S}_d, j \in \mathcal{S}_c, t \in \mathcal{T} \qquad (6)$$

$$\sum_{d \in \mathcal{D}} \sum_{v \in \mathcal{M}_2} \delta_{dj}^{v2t} + \sum_{s \in \mathcal{S}_d} \sum_{v \in \mathcal{M}_2} \epsilon_{sj}^{vt} \leq (1 - \gamma_i^{2t}) A^2 \qquad j \in \mathcal{S}_c, t \in \mathcal{T} \qquad (7)$$

$$\sum_{k \in \mathcal{K}} \sum_{v \in \mathcal{M}_k} \delta_{djv}^{kt} \leq \gamma_d^{1t} A^1 \qquad d \in \mathcal{D}, j \in \mathcal{C}, t \in \mathcal{T} \qquad (8)$$

$$\sum_{v \in \mathcal{M}_2} \epsilon_{sj}^{vt} \leq \gamma_s^{2t} A^2 \qquad s \in \mathcal{S}_d, j \in \mathcal{C}, t \in \mathcal{T} \qquad (9)$$

$$\sum_{d \in \mathcal{D}} \left(\sum_{k \in \mathcal{K}} \sum_{v \in \mathcal{M}_k} \delta_{djv}^{kt} + \sum_{s \in \mathcal{S}_d} \sum_{w \in \mathcal{M}_2} \epsilon_{sj}^{wt} \right) \leq \left(1 - \gamma_d^{1t}\right) A^1 \qquad j \in \mathcal{C}, t \in \mathcal{T} \qquad (10)$$

$$\sum_{d \in \mathcal{D}} \sum_{k \in \mathcal{K}} \sum_{v \in \mathcal{M}_k} \delta_{djv}^{kt} + \sum_{s \in \mathcal{S}_d} \sum_{w \in \mathcal{M}_2} \epsilon_{sj}^{wt} \geq \left(1 - \gamma_m^{1t} - \gamma_n^{2t}\right) D_j^t \qquad m \in \mathcal{D}, n \in \mathcal{S}_d, j \in \mathcal{C}, t \in \mathcal{T} \qquad (11)$$

$$\sum_{k \in \mathcal{K}} \sum_{v \in \mathcal{M}_k} \sum_{j \in \mathcal{C} \cup \mathcal{S}_c} \delta_{djv}^{kt} + \gamma_d^{1t} D_d^t \leq \iota_d^{1t} \qquad d \in \mathcal{D}, t \in \mathcal{T} \qquad (12)$$

$$\sum_{j \in \mathcal{C}} \sum_{v \in \mathcal{M}_2} \epsilon_{sj}^{vt} \leq \iota_s^{2t} \qquad s \in \mathcal{S}_d, t \in \mathcal{T} \qquad (13)$$

$$\sum_{j \in \mathcal{C} \cup \mathcal{S}_c} \delta_{djv}^{kt} \leq G^k \qquad d \in \mathcal{D}, v \in \mathcal{M}_k, k \in \mathcal{K}, t \in \mathcal{T}. \qquad (14)$$

Constraints (2)–(14) deal with the allocation of customers and the opening of facilities. Constraints (2) and (3) prevent terminals and satellites to be opened at nodes where they cannot be constructed. Constraints (4) imply that only one of both facility types can be open at a node. Constraints (5) ensure that an open facility stays open for all future time periods while constraints (6) set any satellite facility with a bunker barge sea side and tanker truck road side. Constraints (7) ensure that a satellite is served by an LNG bunker ship, by prohibiting LNG tanker trucks to serve this demand. Constraints (8) and (9) ensure that customer demand is allocated to open facilities. Constraints (10) ensure that the demand of a node is satisfied if there is a terminal installed at this location. Constraints (11) allocate customer demand to a facility whenever there is no terminal or satellite built at the demand point. Constraints (12) and (13) ensure sufficient facility capacity to satisfy demand, while (14) ensure that vehicle capacities are respected.

$$\theta_s^t + \sum_{d\in\mathcal{D}}\sum_{k\in\mathcal{K}}\sum_{v\in\mathcal{M}_k}\delta_{ds}^{vkt} + \sum_{w\in\mathcal{M}_2}\left(\sum_{u\in\mathcal{S}_d}\epsilon_{us}^{wt} - \sum_{j\in\mathcal{C}}\epsilon_{lj}^{wt}\right) - \left(1-\gamma_s^{1t}\right)D_s^t = \theta_s^{t+1} \qquad s\in\mathcal{S}_c, l\in\mathcal{S}_d, t\in\mathcal{T} \tag{15}$$

$$\theta_s^t \le \iota_s^{1t} \qquad s\in\mathcal{S}_d, t\in\mathcal{T} \tag{16}$$

$$\gamma_d^{et}B^e + \zeta_d^{et}C^e = \iota_d^{et} \qquad d\in\mathcal{D}\cup\mathcal{S}_d, e\in\mathcal{F}, t\in\mathcal{T} \tag{17}$$

$$A^e \ge \iota_d^{et} \qquad d\in\mathcal{D}\cup\mathcal{S}_d, e\in\mathcal{F}, t\in\mathcal{T} \tag{18}$$

$$\zeta_d^{et} \ge \zeta_d^{e,t-1} \qquad d\in\mathcal{D}\cup\mathcal{S}_d, e\in\mathcal{F}, t\in\mathcal{T} \tag{19}$$

$$I^{ek} + \eta^{ekt} = \kappa^{ekt} \qquad e\in\mathcal{F}, k\in\mathcal{K}, t\in\mathcal{T} \tag{20}$$

$$R^{ek} \ge \kappa_k^{et} \qquad e\in\mathcal{F}, k\in\mathcal{K}, t\in\mathcal{T} \tag{21}$$

$$\eta_i^{et} \ge \eta_i^{e,t-1} \qquad e\in\mathcal{F}, k\in\mathcal{K}, t\in\mathcal{T}. \tag{22}$$

Constraints (15)–(22) control the facility inventory, capacity and fleet size. Constraints (15) are inventory conservation and (16) define inventory capacity. Constraints (17) track and update the facility sizes while constraints (18) bound their capacities. Constraints (19) impose that a facility can only be upgraded. Similarly to the constraints regarding facility sizes, the fleet size of both types of vehicles are controlled via constraints (20)–(22), which update the fleet size, set a maximum fleet size and impose that downgrading is not allowed.

$$\sum_{j\in\mathcal{N}}\left(\alpha_{djd}^{vkt} + \alpha_{jdd}^{vkt}\right)G^k - 2\delta_{djv}^{kt} \ge 0 \qquad d\in\mathcal{D}, v\in\mathcal{M}1_k, k\in\mathcal{K}, t\in\mathcal{T} \tag{23}$$

$$\sum_{j\in\mathcal{N}}\left(\alpha_{ijd}^{vkt} + \alpha_{jid}^{vkt}\right)G^k - 2\delta_{div}^{kt} \ge 0 \qquad d\in\mathcal{D}, i\in\mathcal{C}, v\in\mathcal{M}, k\in\mathcal{K}, t\in\mathcal{T} \tag{24}$$

$$\sum_{d\in\mathcal{D}}\sum_{i\in\mathcal{D}}\sum_{j\in\mathcal{N}}\alpha_{ijd}^{vkt} \le 1 \qquad v\in\mathcal{M}_k, k\in\mathcal{K}, t\in\mathcal{T} \tag{25}$$

$$\sum_{j\in\mathcal{N}}\left(\alpha_{ijd}^{vkt} - \alpha_{jid}^{vkt}\right) = 0 \qquad d\in\mathcal{D}, i\in\mathcal{N}, v\in\mathcal{M}_k, k\in\mathcal{K}, t\in\mathcal{T} \tag{26}$$

$$\sum_{j\in\mathcal{N}}\alpha_{ijd}^{vkt} \le 1 \qquad d\in\mathcal{D}, i\in\mathcal{N}, v\in\mathcal{M}_k, k\in\mathcal{K}, t\in\mathcal{T} \tag{27}$$

$$\sum_{j\in\mathcal{N}}\alpha_{jid}^{vkt} \le 1 \qquad d\in\mathcal{D}, i\in\mathcal{N}, v\in\mathcal{M}_k, k\in\mathcal{K}, t\in\mathcal{T} \tag{28}$$

$$\alpha_{ijd}^{vkt} \le L_{ij}^k \qquad i,j\in\mathcal{N}, d\in\mathcal{D}, v\in\mathcal{M}1_k, k\in\mathcal{K}, t\in\mathcal{T} \tag{29}$$

$$\sum_{d\in\mathcal{D}}\sum_{j\in\mathcal{N}}\sum_{v\in\mathcal{M}_k}\alpha_{djd}^{vkt} \le \kappa^{ekt} \qquad k\in\mathcal{K}, t\in\mathcal{T} \tag{30}$$

$$\sum_{j\in\mathcal{N}} \left(\beta_{sj}^{vt} + \beta_{js}^{vt}\right) G^2 - 2\epsilon_{sj}^{vt} \geq 0 \qquad s \in \mathcal{S}_d, v \in \mathcal{M}_k, t \in \mathcal{T} \qquad (31)$$

$$\sum_{j\in\mathcal{N}} \left(\beta_{ijs}^{vt} + \beta_{jis}^{vt}\right) G^2 - 2\epsilon_{si}^{vt} \geq 0 \qquad s \in \mathcal{S}_d, i \in \mathcal{C}, v \in \mathcal{M}_2, t \in \mathcal{T} \qquad (32)$$

$$\sum_{s\in\mathcal{S}_d} \sum_{i\in\mathcal{S}_d} \sum_{j\in\mathcal{N}} \beta_{ijs}^{vt} \leq 1 \qquad v \in \mathcal{M}_2, t \in \mathcal{T} \qquad (33)$$

$$\sum_{j\in\mathcal{N}} \left(\beta_{ijs}^{vt} - \beta_{jis}^{vt}\right) = 0 \qquad s \in \mathcal{S}_d, i \in \mathcal{N}, v \in \mathcal{M}_2, t \in \mathcal{T} \qquad (34)$$

$$\sum_{j\in\mathcal{N}} \beta_{ijs}^{vt} \leq 1 \qquad s \in \mathcal{S}_d, i \in \mathcal{N}, v \in \mathcal{M}_2, t \in \mathcal{T} \qquad (35)$$

$$\sum_{j\in\mathcal{N}} \beta_{jis}^{vt} \leq 1 \qquad s \in \mathcal{S}_d, i \in \mathcal{N}, v \in \mathcal{M}_2, t \in \mathcal{T} \qquad (36)$$

$$\beta_{ijs}^{vt} \leq L_{ij}^2 \qquad i, j \in \mathcal{N}, s \in \mathcal{S}_d, v \in \mathcal{M}_2, t \in \mathcal{T} \qquad (37)$$

$$\sum_{d\in\mathcal{S}_d} \sum_{j\in\mathcal{N}} \sum_{v\in\mathcal{M}_2} \beta_{djd}^{vt} \leq \kappa^{22t} \qquad t \in \mathcal{T} \qquad (38)$$

Constraints (23)–(38) manage the routing part of the problem. Constraints (23) impose that a primary route must start and end at the same terminal. Constraints (24) force to visit every allocated demand point and constraints (25) exclude terminals, other than the allocated one, from being present in the route. Constraints (26) ensure the route flow and constraints (27) and (28) impose a limit of maximum one leaving and one incoming arc per vehicle in a node. Constraints (29) prohibit road vehicles to travel on the waterway network and vice-versa. Constraints (30) prevent using more vehicles than there are available in the fleet. Constraints (31)–(38) act in a similar way for the satellites.

$$\delta_{dj}^{vkt} \geq E^k \delta_{bin}{}_{dj}^{vkt} \qquad d \in \mathcal{D}, j \in \mathcal{C}, v \in \mathcal{M}_k, k \in \mathcal{K}, t \in \mathcal{T} \qquad (39)$$

$$\delta_{dj}^{vkt} \leq G^k \delta_{bin}{}_{dj}^{vkt} \qquad d \in \mathcal{D}, j \in \mathcal{C}, v \in \mathcal{M}_k, k \in \mathcal{K}, t \in \mathcal{T} \qquad (40)$$

$$\epsilon_{sj}^{vt} \geq E^2 \epsilon_{bin}{}_{sj}^{vt} \qquad s \in \mathcal{S}_d, j \in \mathcal{C}, v \in \mathcal{M}_2, t \in \mathcal{T} \qquad (41)$$

$$\epsilon_{sj}^{vt} \leq G^2 \epsilon_{bin}{}_{sj}^{vt} \qquad s \in \mathcal{S}_d, j \in \mathcal{C}, v \in \mathcal{M}_2, t \in \mathcal{T} \qquad (42)$$

Two binary decision variables $\delta_{bin}{}_{dj}^{vkt}$ and $\epsilon_{bin}{}_{sj}^{vt}$ are introduced to impose minimum shipment constraints. These variables are equal to 1 when demand point is allocated, and 0 otherwise. Constraints (39)–(42) impose minimum and maximum delivery quantities.

$$\sum_{d\in\mathcal{S}_d} \sum_{j\in\mathcal{N}} \sum_{v\in\mathcal{M}_k} \sum_{k\in\mathcal{K}} \mu_{djd}^{vkt} = \sum_{d\in\mathcal{D}} \sum_{j\in\mathcal{N}} \sum_{v\in\mathcal{M}_k} \sum_{k\in\mathcal{K}} \delta_{dj}^{vkt} \qquad t \in \mathcal{T} \qquad (43)$$

$$\sum_{j\in\mathcal{N}} \mu_{jid}^{vkt} - \sum_{j\in\mathcal{N}} \nu_{ijd}^{vkt} = \delta_{di}^{vkt} \qquad d \in \mathcal{D}, i \in \mathcal{C}, v \in \mathcal{M}_k, k \in \mathcal{K}, t \in \mathcal{T} \qquad (44)$$

$$\mu_{idd}^{vkt} = 0 \qquad d \in \mathcal{D}, i \in \mathcal{N}, v \in \mathcal{M}_k, k \in \mathcal{K}, t \in \mathcal{T} \qquad (45)$$

$$\sum_{s\in\mathcal{S}_d} \sum_{j\in\mathcal{N}} \sum_{v\in\mathcal{M}_2} \nu_{sjs}^{vt} = \sum_{s\in\mathcal{S}_d} \sum_{j\in\mathcal{N}} \sum_{v\in\mathcal{M}_2} \epsilon_{sj}^{vt} \qquad t \in \mathcal{T} \qquad (46)$$

$$\sum_{j\in\mathcal{N}} \nu_{jis}^{vt} - \sum_{j\in\mathcal{N}} \nu_{ijs}^{vt} = \epsilon_{si}^{vt} \qquad s \in \mathcal{S}_d, i \in \mathcal{C} \setminus s, v \in \mathcal{M}_2, t \in \mathcal{T} \qquad (47)$$

$$\nu_{iss}^{vt} = 0 \qquad s \in \mathcal{S}_d, i \in \mathcal{N}, v \in \mathcal{M}_2, t \in \mathcal{T}. \tag{48}$$

Subtours in the routes of both types of vehicles are eliminated using commodity flow constraints (43)–(48) [Lahyani et al., 2018]. Two new decision variables μ_{ijd}^{vkt} and ν_{ijs}^{vt} are introduced for the routes of the primary and secondary vehicles respectively. These variables represent the load on the vehicle v of type k starting from a facility traversing edge (i, j). Constraints (43) ensure that the sum of all allocated demand leaves the depot and constraints (44) ensure that the weight load decreases when a demand point is satisfied. Constraints (45) impose that the final load going back to the depot is equal to 0. Constraints (46)–(48) are similar for the fleet serving satellites only.

$$\sum_{d \in \mathcal{D}} \sum_{i \in \mathcal{C}} \left(\delta_{di}^{vkt} - \delta_{di}^{v-1kt}\right) \leq 0 \qquad v \in \mathcal{M}_k \setminus 1, k \in \mathcal{K}, t \in \mathcal{T} \tag{49}$$

$$\sum_{s \in \mathcal{S}_d} \sum_{i \in \mathcal{C}} \left(\epsilon_{si}^{vt} - \epsilon_{si}^{v-1t}\right) \leq 0 \qquad v \in \mathcal{M}_2 \setminus 1, t \in \mathcal{T} \tag{50}$$

$$\delta_{lin}{}_{dj}^{vkt} \leq G^k \gamma_i^{et} \qquad d \in \mathcal{D}, j \in \mathcal{C}, v \in \mathcal{M}_k, k \in \mathcal{K}, t \in \mathcal{T} \tag{51}$$

$$\delta_{lin}{}_{dj}^{vkt} \leq \delta_{dj}^{vkt} \qquad d \in \mathcal{D}, j \in \mathcal{C}, v \in \mathcal{M}_k, k \in \mathcal{K}, t \in \mathcal{T} \tag{52}$$

$$\delta_{lin}{}_{dj}^{vkt} \geq \delta_{dj}^{vkt} - \left(1 - \gamma_i^{et}\right) G^k \qquad d \in \mathcal{D}, j \in \mathcal{C}, v \in \mathcal{M}1_k, k \in \mathcal{K}, t \in \mathcal{T}. \tag{53}$$

The formulation of the model can be further tightened by adding symmetry breaking constraints. Constraints (49) and (50) are symmetry breaking constraints for the routes of both types of vehicles respectively. The use of constraints (51), (52) and (53) significantly decreases computing time. A new continuous decision variable δ_{lin} is introduced which represents the amount of LNG transported from a terminal to a satellite, i.e., an indirect shipment. This amount of LNG shall be stored temporarily in a satellite.

$$\alpha_{ijd}^{vkt}, \beta_{ijs}^{vt}, \gamma_{ie}^{t}, \delta_{bin_{dj}}^{vkt}, \epsilon_{bin_{sj}}^{vt} \in \{0, 1\} \tag{54}$$

$$\delta_{ijv}^{kt}, \epsilon_{ij}^{vt}, \iota_{ie}^{t}, \kappa_{ek}^{t} \geq 0 \tag{55}$$

$$\zeta_{ie}^{t}, \eta_{ie}^{t}, \theta_{i}^{t} \in \mathbb{N}. \tag{56}$$

Constraints (54)–(56) define the domain of the decision variables.

3 Solution algorithm

In this section we describe the algorithm used to solve the problem and several improvements we have made to it. This algorithm is inspired in the variable MIP neighborhood descent (VMND) of Larrain et al. [2017]. This algorithm is described in Section 3.1, after which improvement opportunities are described in Section 3.2. In Section 3.3 we show how to apply this algorithm to the problem at hand.

3.1 Description of the variable MIP neighborhood descent algorithm

VMND was introduced to solve an inventory management and vehicle routing problem arising in the cash logistics industry, and is based on formulating the problem as a MIP, which is then solved with several heuristic rules, such as in a fix-and-optimize framework. Such a structure allows for quickly obtaining primal solutions, while still retaining dual information, thus being able to prove optimality and/or to compute the gap of a solution. Hence, VMND is an exact algorithm, which alternates between two phases, a local search phase and an exact phase.

During the local search phase, the main problem is restricted by new constraints, i.e., performing a local search similar to a Variable Neighborhood Search (VNS) [Mladenović and Hansen, 1997]. In the local search phase, different neighborhoods are explored using the best improvement heuristic. The solution of the best improvement is given back to the exact phase as a starting solution, which significantly increases its performance. The exact phase is limited by the amount of time that the algorithm spent in the local search phase. When a new incumbent solution is found, or the time limit has been exceeded, the algorithm switches back to the local search phase.

3.2 Improvement opportunities

Three opportunities have been identified in order to increase performance of the described algorithm. The first one relates to the number of times one alternates between the two phases. Initially, VMND is designed to switch from the local search phase to the exact phase when an improved solution is found in a neighborhood. This results in an equal amount of runs of the exact phase and the number of improvements found in the local search phase. This is beneficial for small problems for which the exact phase is easy and not very time consuming. However, when the size of the problem increases due to a larger network size, number of demand points, vehicles or candidate facility locations, the model size increases and the exact phase will take significantly longer. Therefore, a first improvement is to change neighborhoods similar to a Basic VNS as described in Duarte et al. [2016]. This will decrease the number of alternations while improving the best found solution. The benefit will also come from the reduced time spent in the exact phase.

Secondly, when the algorithm does not improve the solution in the exact phase, the local search phase takes over. However, this is not beneficial when an optimal solution value is already obtained, and thus no further improvement is possible. This occurs when the solution has reached an optimal value, but an optimality gap still exists. Therefore, when the best solution from both phases is equal, one should not stop the exact phase and switch back to the local search phase unless a new solution has been found.

The third identified opportunity is to decrease the amount of redundant time spent in neighborhoods. During the exploration of neighborhoods, a significant proportion of computing time can be devoted to decreasing the relative MIP gap from, say, 2% to 0%. It can be empirically observed that there is little to no added value for the last explorations

when no improvement is found. For this reason, two new parameters have been added to the algorithm which cut off the exploration of neighborhoods. The first parameter is a time limit and the second one is a relative MIP gap tolerance for exploring neighborhoods, denoted as β and γ, respectively. Figure 1 visualizes the new algorithm.

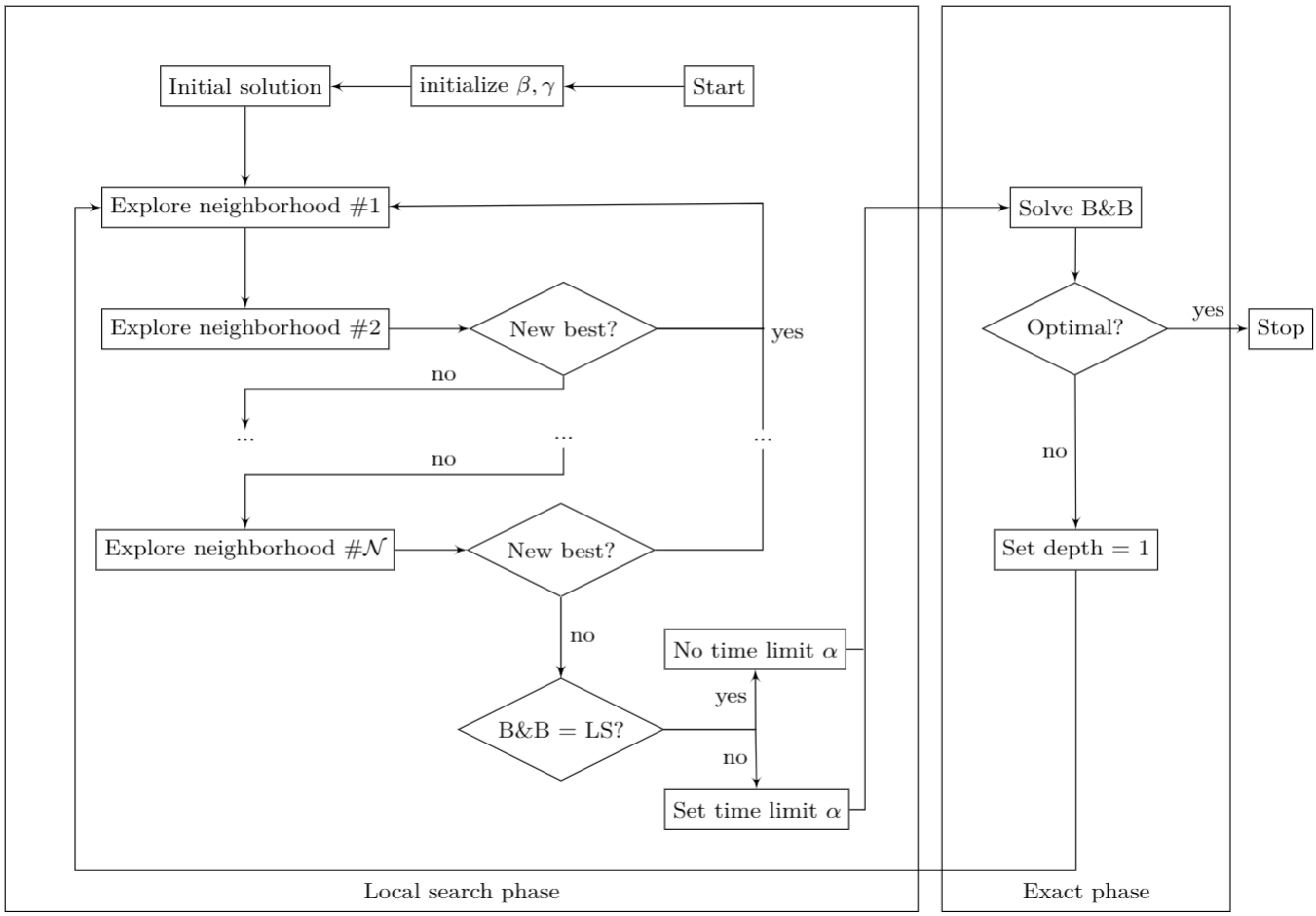

Figure 1: Improved VMND algorithm

3.3 Applying the improved VMND to the 2E-CLRPSP

We have designed five neighborhoods based on the structure of the problem. These are meant to allow the algorithm to change all decisions variables while not yielding too difficult MIPs. The neighborhoods together with their defining operations are:

1. *Route:* changing one route of one vehicle in one time period. This neighborhood fixes the routes of all vehicles except one, and iterates over all vehicles and periods.

2. *Vehicles:* changing the routes of one specific vehicle across all periods. Here, we allow one vehicle to be kept free over all the planning horizon, while the routes of all other vehicles are fixed.

3. *Periods:* changing all variables in two periods. We take every pair of periods and let all their associated variables be free.

4. *Satellites:* changing one terminal and two satellites across all periods. Here, we allow more flexibility by exploring the interactions among three facilities, being one terminal and a pair of satellites.

5. *All Routes:* changing all routes but one across all periods. Unlike the Route neighborhood, here we fix one route at a time and let all others be free.

A neighborhood is defined as the solutions that can be reached by applying an operator to a given solution. Every neighborhood $n \in \mathcal{N}$ has an associated set of valid parameterizations $\mathcal{P}_n$. A parameterized neighborhood is denoted as n_p with parameters $p \in \mathcal{P}_n$. One parameterizaion of neighborhood "Route" could be $v = 2$, $k = 1$ and $t = 3$ which allows the model to change the route of the second bunker barge (vehicle type $k = 1$) in the third time period. All other routes are fixed in the current solution.

The developed neighborhoods differ in size and complexity. In order to provide an estimate of the complexity of the subproblem, the *MIP size* is given. The MIP size is the upper bound to the number of free variables per individual decision variable in a neighborhood. Using the MIP size, the complexity of a neighborhood can be calculated by multiplying the MIP size times the amount of possible combinations $\mathcal{P}_n$ in the neighborhood. Table 1 describes the neighborhoods with its characteristics.

Table 1: Neighborhood definitions

n	Neighborhood	$\mathcal{P}_n$	p	MIP size
1	Route	$\mathcal{M} \times \mathcal{K} \times \mathcal{T}$	(v_p, k_p, t_p)	E
2	Vehicles	$\mathcal{M} \times \mathcal{K}$	(v_p, k_p)	ET
3	Periods	$\mathcal{T}$	$(t1_p, t2_p)$	$2EKSM$
4	Satellites	$\mathcal{D} \times (\mathcal{S} \times \mathcal{S}_{-1})/2$	$(d_p, s1_p, s2_p)$	$2EKTM$
5	All Routes	$\mathcal{M} \times \mathcal{K}$	(v_p, k_p)	$EKDSMT$

Each neighborhood can be seen as a new subproblem that results in a local optimal solution when solved. Neighborhoods "Route" and "Vehicles" can be defined as LRPs with one vehicle with semi-fixed facilities;"Periods" as a 2E-LRP with two periods; "Satellites" as a 2E-LRP with one terminal and two satellites; and "All Routes" as a 2E-LRP with semi-fixed facilities. Facilities are said to be semi-fixed, as the decision variable γ handling opening of a facility is free. However, fixed variables such as routing can imply an open facility. Table 2 shows the fixed variables for each neighborhood.

Table 2: Fixed values in neighborhoods

Variable	Route	Vehicles	Periods	Satellites	All Routes
α_{ijd}^{vkt}	$t \neq t_p$	$k \neq k_p$	$t \neq t_p$	Free	$v = v_p$
	$k \neq k_p$	$v \neq v_p$			$k = k_p$
	$v \neq v_p$				
β_{ijs}^{vt}	$t \neq t_p$	$k \neq k_p$	$t \neq t_p$	Free	$v = v_p$
	$k \neq k_p$	$v \neq v_p$			
	$v \neq v_p$				
γ_i^{et}	Free	Free	Free	$i \neq i_p$	Free
				$e \neq 2$	
δ_{dj}^{vkt}	$t \neq t_p$	$k \neq k_p$	$t \neq t_p$	Free	Free
	$k \neq k_p$	$v \neq v_p$			
	$v \neq v_p$				
ϵ_{sj}^{vt}	$t \neq t_p$	$k \neq k_p$	$t \neq t_p$	Free	Free
	$k \neq k_p$	$v \neq v_p$			
	$v \neq v_p$				
ζ_i^{et}	Free	Free	Free	Free	Free
η^{ekt}	Free	Free	Free	Free	Free
θ_i^t	Free	Free	Free	Free	Free
ι_i^{et}	Free	Free	Free	Free	Free
κ^{ekt}	Free	Free	Free	Free	Free

4 Computational experiments

In this section extensive computational experiments are presented. In Section 4.1 we describe the data related to the instances we created to evaluate our algorithm. In Section 4.2 we performed detailed sensitivity analysis on the parameters and neighborhoods of our algorithm to determine the best combination. In Section 4.3 we assess the performance of our algorithm against the original VMND of Larrain et al. [2017] and against a state-of-the-art solver. Finally, we solve a case study for the European LNG network in Section 5.

The algorithms were coded in C++ and we have used CPLEX 12.7 as the MIP solver. Unless otherwise specified, all tests were executed with a time limit of 3 hours.

4.1 Instances description

We have generated 26 instaces by varying the number of terminal locations (D), satellite locations (S), demand points (C), and time periods (T). An instance is then characterized by its configurations $D/S/C/T$. The individual parameters are similar to those of the LNG case, which have been confirmed by the industry. The largest instances are of similar size as the case study depicted later, such that the algorithm can be used for obtaining better results in the real-life case. All costs are measured in Euros.

4.2 Sensitivity analysis on the time limit and optimality gap parameters of the local search

We now assess the performance of the algorithm with respect to how long we allow the subproblems arising in the local search to be solved, and optimality gap that must be achieved before the problem is deemed solved. These are the two new parameters we introduce to the algorithm. To this end, the base case allows each subproblem to be solved for up to 1000 seconds, or when optimality has been proved at 0.00% gap.

We select a subset of 10 instances ranging from all sizes and we allow the time limit β and the relative gap tolerance γ to vary. The results of this test are used to guide how to order the neighborhoods and to define suitable values for β and γ.

4.2.1 Time limit β

In order to test the influence of the time limit parameters, three different input values are given for β: 10, 20 and 50 seconds.

The quality of the results depicted in Table 3 show a high dependency on the complexity of the newly created subproblem. The smaller and less complex neighborhoods "Route", "Vehicles" and "Periods" show little impact on their behavior. This is due to the low complexity of the problem and the relatively high time limit for these specific neighborhoods. The time limit is only exceeded in the last iteration of the local search phase for these relatively small problems.

A greater impact is seen in neighborhoods with a higher level of complexity, such as in "Satellites" and "All Routes". The local search phase is then truncated. This can lead to less redundant computations and therefore increased performance. However, it must be noted that a time limit that is set too low, can lead to low quality solutions and therefore decrease the exact phase performance. This can be seen in neighborhood "Periods" and "Satellites".

Table 3 shows the decrease in computing time for the different input values. A positive value reflects a decrease in computing time compared to the default case, while a negative value points to an increase in computation time.

Table 3: Average decrease in computing times compared to $\beta = 1000$s

β	Route	Vehicles	Periods	Satellites	All Routes	Average
10s	16.82%	5.81%	-9.94%	55.42%	32.60%	20.14%
20s	3.89%	4.68%	-3.63%	5.25%	41.71%	10.38%
50s	-1.10%	4.67%	3.97%	-6.56%	9.02%	2.00%

The influence of the time limit can also be observed on the behavior of the solution over time. Figure 2a shows two typical behaviors related to a low time limit, applied to a typical instance. The first phenomenon that can be observed is that a low time limit can negatively influence the neighborhoods' ability to quickly decrease the objective value. This can result in fewer new solutions and a higher upper bound in the local search phase. This can potentially lead to longer computing times in the exact phase.

The second phenomenon shows a beneficial characteristic for the low time limit. After some time, the low time limit can outperform the default case. The local search takes longer as the relative gap in the exact phase is becoming smaller. Therefore, the time limit will mainly cut the local search later in the algorithm. A similar behavior is observed for another neighborhood in Figure 2b.

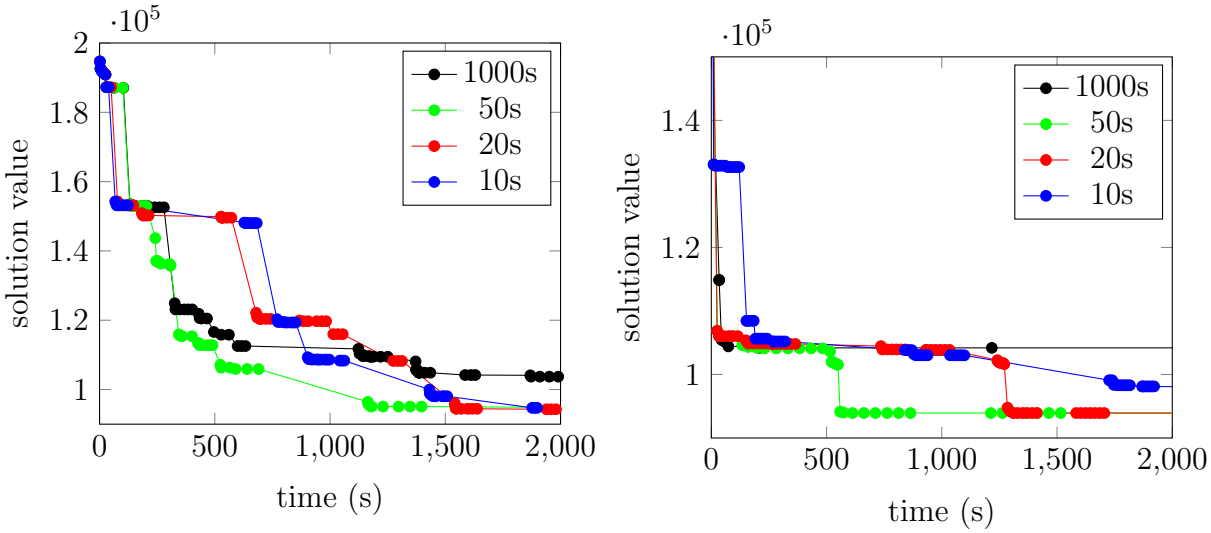

(a) Neighborhood "Periods"

(b) Neighborhood "Satellites"

Figure 2: The behavior related to the time limit β of two neighborhoods in instance 26

The test results show that it can be beneficial to lower the time limit such that long neighborhood explorations are eliminated. As the complexity of each neighborhood varies, setting a low time limit can help finish the execution of a more complex neighborhood, while it will have no effect in a smaller neighborhood. The time limit can be used in such a way that it operates as the upper bound of the largest neighborhood.

4.2.2 Relative gap tolerance γ

The relative gap tolerance limit γ restricts the exploration of a neighborhood up until the set value. The behavior is tested on four values of γ: 2%, 5%, 10% and 20%.

Tests show that the relative gap limit improves performance in all cases. The lowest value of γ results in the worst average performance and decreases the average computing time by 41% when compared to the default case. The best average performance results from a limit value set to 10%. This decreases the average running times by 60% and consistently decreases running times in all neighborhoods by more than 40%. The lower performance of the lowest set value is due to longer computing times in the local search phase. A higher value of γ can also result in decreased performance. This happens when the tolerance is too high and does not allow the neighborhood to converge and find new solutions. Table 4 shows the decrease in computing times for the subset of tested instances.

Table 4: The decrease in computing times compared to $\gamma = 0\%$

Value of γ	Route	Vehicles	Periods	Satellites	All Routes	Average
0.02	61.86%	37.41%	33.54%	16.59%	59.30%	41.74%
0.05	72.85%	52.95%	42.56%	60.24%	56.23%	56.97%
0.10	53.86%	57.86%	43.67%	82.06%	63.75%	60.24%
0.20	56.97%	57.90%	43.31%	15.30%	58.95%	46.48%

Figure 3 shows the behavior of neighborhoods Satellites and Periods applied to a typical instance. It can be seen from Figure 3b that most variations outperform the default case. The long and extensive local searches are cut off which allows the exact phase to find a new better solution. Figure 3a shows a behavior in which the lowest set value is the weakest performer, after the default case. In this case, the lower quality solutions given to the exact phase result in a weaker performance of that phase.

The relative gap tolerance limit can eliminate excessive neighborhood exploration and significantly increase performance. It must be choosen in such a way that it is not too low that it will not exhaust neighborhoods and not too high such that valuable information is lost.

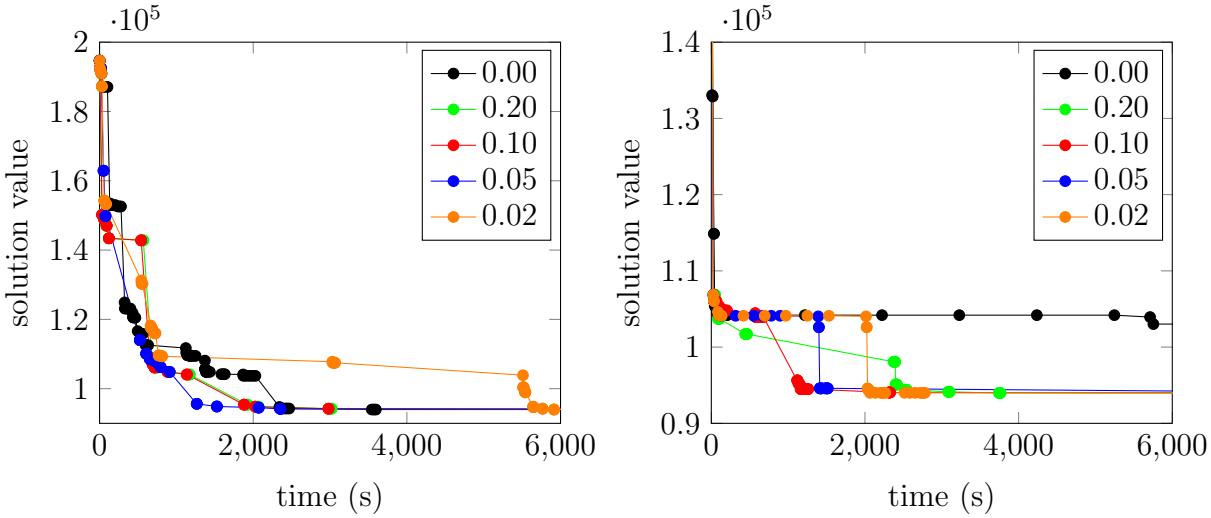

(a) Neighborhood "Periods"

(b) Neighborhood "Satellites"

Figure 3: The behavior related to the time limit γ of two neighborhoods in instance 26

4.3 Detailed computational results

In this section the results on 26 instances are shown and discussed. The instances are solved using CPLEX, the original algorithm structure of Larrain et al. [2017] and the new improved algorithm we propose. For each instance, an identical initial solution is given for the three methods. First, the results of the former algorithm are compared with standard CPLEX. Hereafter, the results of the former algorithm are compared with the

new algorithm to show that the former algorithm has been improved. Finally the results of CPLEX are compared with the improved algorithm such that it can be seen that the proposed algorithm outperforms standard CPLEX.

The final algorithm includes 4 neighborhoods which are ordered as follows; 1. Vehicles, 2. Routes, 3. Periods, 4. Satellites. The number of neighborhoods has been decreased from 6 to 4 in order to decrease redundant time in the local search. The sequence of the neighborhoods is based on the results of Section 4.2.1 and 4.2.2 and on increasing neighborhood complexity. It must be noted that the first neighborhood "Vehicles" is more complex than the second "Routes", for increasing the speed in the first iteration. Two columns will be introduced to compare methods with one another. Column "G Diff" shows the absolute decrease in the relative MIP gap, i.e., a gap that decreases from 10% to 5% has a 5% absolute decrease. Column "T Diff" shows the relative decrease in computation time, i.e., a time that decreases form 100 to 40 seconds has a 60% relative decrease. Note that a positive value points to an improvement while a negative value is not desired.

4.3.1 Results from CPLEX

Table 5 shows the results on all 26 instances using standard CPLEX. The CPLEX method is not able to obtain solutions for instances 9, 14 and 17 within three hours and instances 10, 18, 19, 20 and 21 are solved optimally.

4.3.2 Former algorithm vs CPLEX

Table 6 shows the results on all 26 instances executed by the former algorithm. The value for α is set to 1. Since there are no parameters β and γ included in the former algorithm, values are set to 1000 seconds (unlimited) and 0%, respectively. It can be seen that the algorithm did not find a lower bound for instance 9 since the algorithm searches for solutions in the local search which prevent the B&B phase to compute a lower bound. The former algorithm has been able to compute a solution for all instances and solved optimally for instances 10, 18, 19, 20, 21, 22 and 23, this already better than CPLEX.

The former algorithm has been able to compute a solution for three instances for which CPLEX did not provide a solution. Also, two more instances were solved optimally using the former algorithm. The results show that optimal solutions were computed using 33% less time on average. The performance on larger instances was less beneficial as the relative gap increased by 7.8% on average. This performance characteristic was already acknowledged in Larrain et al. [2017]. It can be stated that the former algorithm is beneficial for small instances. When the instance sizes become larger, its efficiency decreases.

4.3.3 New algorithm vs former algorithm

In the new algorithm, the values of β and γ have been changed to 50 seconds and 0.05 respectively. These values are chosen based on the results from Section 4.2.1 and 4.2.2.

Table 5: Results of the CPLEX algorithm

#	Scenario	Upper bound	Lower bound	Gap (%)	Time (s)
1	2/2/2/2	79360	78821	0.68	10800
2	2/2/2/4	88940	87490	1.63	10800
3	2/2/2/6	105740	64593	38.91	10800
4	2/2/6/2	95170	94105	1.12	10800
5	2/2/6/4	115800	103866	10.31	10800
6	2/2/6/6	217640	80477	63.02	10800
7	2/2/10/2	80580	79895	0.85	10801
8	2/2/10/4	142380	129002	9.40	10800
9	2/2/10/6	–	–	–	10800
10	2/4/2/2	84550	84550	0.00	1207
11	2/4/2/4	155845	89273	42.72	10800
12	2/4/2/6	230745	68132	70.47	10801
13	2/4/6/2	107195	103401	3.54	10801
14	2/4/6/4	–	–	–	10800
15	2/4/6/6	257820	100888	60.87	10801
16	2/4/10/2	128860	117537	8.79	10800
17	2/4/10/4	–	–	–	10800
18	1/1/3/2	66370	66370	0.00	52
19	1/1/3/2	67440	67440	0.00	775
20	1/1/4/2	78560	78560	0.00	4206
21	1/2/2/1	67620	67620	0.00	1753
22	1/2/2/2	83570	82504	1.28	10800
23	1/2/2/3	75860	75172	0.91	10800
24	2/2/2/2	82500	81827	0.82	10800
25	2/2/4/2	88560	86918	1.85	10800
26	2/2/6/2	93980	92395	1.69	10800
Average		112830	86123	17.71	1598

Table 6: Results of the former algorithm compared to CPLEX

#	Scenario	U bound	L bound	Gap (%)	G Diff (%)	Time (s)	T Diff (%)
1	2/2/2/2	79360	79058	0.38	0.30	10800	0.00
2	2/2/2/4	88860	78647	11.49	-9.86	10800	0.00
3	2/2/2/6	97980	85396	12.84	26.07	10800	0.00
4	2/2/6/2	97390	67675	30.51	-29.39	10800	0.00
5	2/2/6/4	115430	71113	38.39	-28.08	10800	0.00
6	2/2/6/6	154480	68808	55.46	7.56	10800	0.00
7	2/2/10/2	80540	77322	4.00	-3.15	10800	0.00
8	2/2/10/4	144370	124442	13.80	-4.40	10800	0.00
9	2/2/10/6	205780	–	–	0.00	10800	0.00
10	2/4/2/2	84550	84550	0.00	0.00	4133	-242.42
11	2/4/2/4	98100	58464	40.40	2.32	10800	0.00
12	2/4/2/6	116650	54886	52.95	17.52	10800	0.00
13	2/4/6/2	119365	65162	45.41	−41.87	10800	0.00
14	2/4/6/4	139885	78298	44.03	−44.03	10800	0.00
15	2/4/6/6	184290	90048	51.14	9.73	10800	0.00
16	2/4/10/2	127660	95839	24.93	−16.14	10800	0.00
17	2/4/10/4	177085	110430	37.64	−37.64	10800	0.00
18	1/1/3/2	66370	66370	0.00	0.00	47	9.62
19	1/1/3/2	67440	67440	0.00	0.00	67	91.35
20	1/1/4/2	78560	78560	0.00	0.00	169	95.98
21	1/2/2/1	67620	67620	0.00	0.00	39	97.78
22	1/2/2/2	83570	83570	0.00	1.28	1677	84.47
23	1/2/2/3	75860	75860	0.00	0.91	587	94.56
24	2/2/2/2	82500	45751	44.54	-43.72	10800	0.00
25	2/2/4/2	88740	81623	8.02	-6.17	10800	0.00
26	2/2/6/2	93980	86159	8.32	-6.63	10800	0.00
	Average	108324	77724	29.12	-11.41	891	33.05

Table 7 shows the results of the new algorithm. It can be seen that an optimal solution has been found for 7 out of 26 instances. For 5 of these instances, the new algorithm outperformed the old algorithm with an average decrease of 63.60% in computation time. Instances 22 and 24 performed worse, with a slight increase of 2.56% and 1.98% respectively. The new algorithm outperforms the old algorithm with an average decrease of 44.84% in computation time.

Table 7: Results of our new improved algorithm compared to the former one

#	Scenario	U bound	L bound	Gap (%)	G Diff (%)	Time (s)	T Diff (%)
1	2/2/2/2	79360	79081	0.35	0.03	10800	0.00
2	2/2/2/4	88860	88019	0.95	10.54	10800	0.00
3	2/2/2/6	97980	96125	1.89	10.95	10800	0.00
4	2/2/6/2	95170	94594	0.61	29.90	10800	0.00
5	2/2/6/4	110710	99430	10.19	28.20	10800	0.00
6	2/2/6/6	139320	83810	39.84	15.62	10800	0.00
7	2/2/10/2	118640	118087	0.47	3.53	10800	0.00
8	2/2/10/4	143980	129849	9.81	3.99	10800	0.00
9	2/2/10/6	190220	–	–	–	10800	0.00
10	2/4/2/2	84550	84550	0.00	0.00	1967	52.41
11	2/4/2/4	98100	93323	4.87	35.53	10800	0.00
12	2/4/2/6	125720	67584	46.24	6.71	10800	0.00
13	2/4/6/2	110125	97899	11.10	34.31	10800	0.00
14	2/4/6/4	141785	88981	37.24	6.79	10800	0.00
15	2/4/6/6	162800	93685	42.45	8.69	10800	0.00
16	2/4/10/2	127150	109699	13.72	11.21	10800	0.00
17	2/4/10/4	167970	114755	31.68	5.96	10800	0.00
18	1/1/3/2	66370	66370	0.00	0.00	23	51.06
19	1/1/3/2	67440	67440	0.00	0.00	13	80.60
20	1/1/4/2	78560	78560	0.00	0.00	98	42.01
21	1/2/2/1	67620	67620	0.00	0.00	40	-2.56
22	1/2/2/2	83570	83570	0.00	0.00	128	92.37
23	1/2/2/3	75860	75860	0.00	0.00	604	-2.90
24	2/2/2/2	82500	82085	0.50	44.04	10800	0.00
25	2/2/4/2	88560	86912	1.86	6.16	10800	0.00
26	2/2/6/2	93930	92334	1.70	6.62	10800	0.00
	Average	107187	89609	9.83	14.93	428	44.71

For the 19 remaining instances, we did not find an optimal value. The performance of the algorithm is then measured using the change in relative gap in column "G Diff". Improvements are seen for all instances. The lowest improvement of 0.03% has been obtained for the first instance which has a low relative gap of 0.38% computed by the former algorithm. The highest attained improvement resulted in 44.04% gap improvement. The gap decreases in every instance with an average decrease of 14.93%. Instance 9 again did not provide a lower bound however, the upper bound decreased by 7.6%.

The results show that the implications as described in this paper result in an overall better performance. The times for computing optimal solutions decreased on average with 44.84% while the relative gaps of the other instances decreased on average with 14.93%.

4.3.4 New algorithm vs CPLEX

Table 8 shows the results of the new algorithm compared to those of CPLEX. Optimal solutions were generated 69% faster on average, with a maximum of 99%. The new algorithm outperformed CPLEX for six instances and performed worse for only one.

Table 8: Results of the new algorithm compared to CPLEX

#	Scenario	U bound	L bound	Gap (%)	G Diff (%)	Time (s)	T Diff (%)
1	2/2/2/2	79360	79081	0.35	0.33	10800	0.00
2	2/2/2/4	88860	88019	0.95	0.68	10800	0.00
3	2/2/2/6	97980	96125	1.89	37.02	10800	0.00
4	2/2/6/2	95170	94594	0.61	0.51	10800	0.00
5	2/2/6/4	110710	99430	10.19	0.12	10800	0.00
6	2/2/6/6	139320	83810	39.84	23.18	10800	0.00
7	2/2/10/2	118640	118087	0.47	0.38	10800	0.00
8	2/2/10/4	143980	129849	9.81	-0.41	10800	0.00
9	2/2/10/6	190220	–	0.00	–	10800	0.00
10	2/4/2/2	84550	84550	0.00	–	1967	-62.97
11	2/4/2/4	98100	93323	4.87	37.85	10800	0.00
12	2/4/2/6	125720	67584	46.24	24.23	10800	0.00
13	2/4/6/2	110125	97899	11.10	-7.56	10800	0.00
14	2/4/6/4	141785	88981	37.24		10800	0.00
15	2/4/6/6	162800	93685	42.45	18.42	10800	0.00
16	2/4/10/2	127150	109699	13.72	-4.93	10800	0.00
17	2/4/10/4	167970	114755	31.68	–	10800	0.00
18	1/1/3/2	66370	66370	0.00	–	23	55.77
19	1/1/3/2	67440	67440	0.00	–	13	98.32
20	1/1/4/2	78560	78560	0.00	–	98	97.67
21	1/2/2/1	67620	67620	0.00	–	40	97.72
22	1/2/2/2	83570	83570	0.00	1.28	128	98.81
23	1/2/2/3	75860	75860	0.00	0.91	604	94.41
24	2/2/2/2	82500	82085	0.50	0.32	10800	0.00
25	2/2/4/2	88560	86912	1.86	-0.01	10800	0.00
26	2/2/6/2	93930	92334	1.70	-0.01	10800	0.00
	Average	107187	89609	9.83	7.35	428	68.53

The relative gap decreased on average by 7.35% in the scenarios that did not provide optimal solutions. The new algorithm outperformed CPLEX on 16 instances.

The new algorithm provided a solution for all instances while CPLEX did not find any solution for three cases. The times for computing optimal solutions decreased on average by 69%, while the relative gaps of the other instances decreased on average by 7.35%.

5 Case study

We apply our algorithm to find solutions for a real-life LNG network design problem. The European Commission, through its Alternative Fuels Directive 2014/94/EU, is seeking to promote the deployment of alternative fuels infrastructure to enable an increase in the

uptake of alternative fuels vehicles. LNG is regarded as a prominent alternative fuel for road and maritime transportation for the near-future, as it is both more environmentally friendly and lower in cost for its end-users, compared to the current transportation fuels. LNG can reduce SO_x emissions with up to 93%, NO_x with up to 50%, and CO_2 with up to 20%. Accordingly, LNG complies with environmental regulations set by the EU [SER, 2014a]. CO_2 emissions can be even further reduced, by up to 80%, when liquefying bio gas, instead of natural gas [Kasper, 2013, Verbeek and Verbeek, 2015]. Lastly, LNG vehicles produce up to 50% less noise, which enables traveling into noise-constrained areas [Zhao et al., 2013].

A rapid uptake of LNG as an alternative fuel requires considerable development of the infrastructure through which it is made available to its end-users. In terms of LNG fuel stations, the European infrastructure has been quickly expanding. The fueling infrastructure for the maritime sector is still somewhat lagging, possibly both the reason for and result of a slower uptake in demand. Thus far, infrastructure development has focused on adjusting ports so that ships can take on LNG from tanker trucks. This so-called truck-to-ship bunkering method is relatively inexpensive at low volumes of LNG, and when the port is located nearby an import terminal. Other bunkering methods require additional specialized resources, which are still in development. In ship-to-ship bunkering, a specially developed bunker barge loads large quantities of the fuel at an import terminal and then meets ships in need of LNG in ports to fuel them. Bunker barges can fuel any ship, at virtually any port without infrastructure changes on the land-side, but is also associated with high investment and operational costs. It is therefore only a viable option in scenarios with strong demand growth. Ships can also be supplied with LNG as a fuel from (satellite) terminals, yet constructing an LNG terminal solely for fueling purposes is not cost-effective.

The European Commission supports LNG infrastructure development with the ambition to foster a rapid uptake of LNG as a fuel for transportation. For the longer-term viability of the market for LNG, it is critically important to make only the necessary investments, as any excess investment will have a negative impact on the price end-users pay for the fuel. A variety of network design decisions are to be considered for achieving these short- and longer-term goals. Strategic decisions are to be made on the possible construction of LNG terminals and satellites. The location and size of the terminal are important aspects in that regard. These facility location decisions are strongly influenced by decisions pertaining to the investment in bunker barges and tanker trucks and the routing of those vehicles when replenishing fuel stations and visiting ports.

5.1 Case description

We rely on several sources of data and observations in practice in creating scenarios that reflect the current and planned development of the small-scale LNG supply chain in Europe. The Netherlands has been a front runner, with 17 LNG fuel stations being operational in 2017, and 12 new stations being developed. So far, 7 port locations were adjusted so that ships can take on LNG from tanker trucks. In our experiment, we

consider a network with 16 demand points distributed over 14 locations. To this end, we create clusters of multiple LNG fuel stations, reflecting geographical regions throughout the network. Figure 4 shows the network, including the division of the waterway demand in % per port and the road demand in number of fuel stations. Note that there are two locations (i.e., the ports of Doesburg and Cologne) where there is both waterway and road demand. In 2017, no satellite terminals were yet in operation, but the development of satellite terminals at the port locations is under consideration.

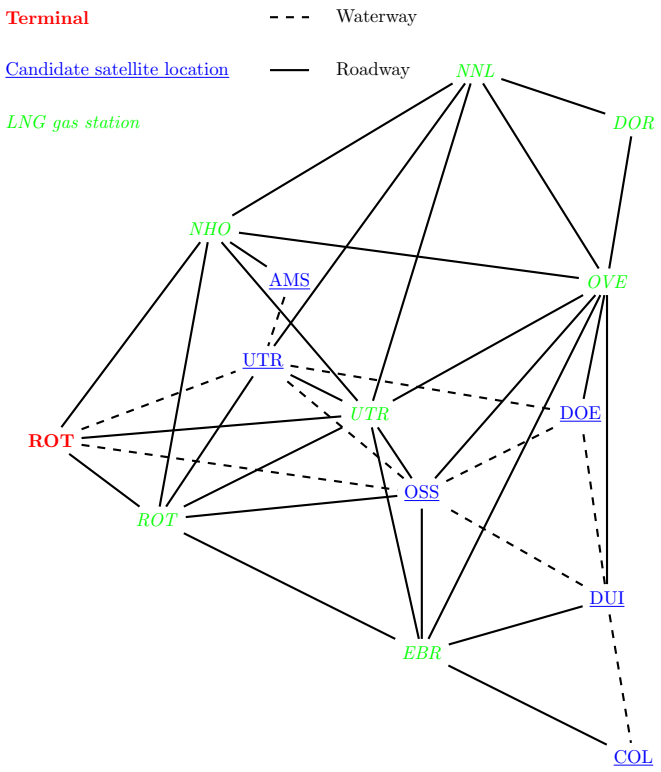

#	Location		% ships	# fuel stations
1	Port of Amsterdam	AMS	20	0
2	Port of Rotterdam	ROT	20	0
3	Port of Duisburg	DUI	20	0
4	Port of Oss	OSS	10	0
5	Port of Utrecht	UTR	10	0
6	Port of Doesburg	DOE	10	1
7	Port of Cologne	COL	10	1
8	North Netherlands	NNL	0	4
9	North Holland	NHO	0	3
10	Utrecht	UTR	0	6
11	Overijssel	OVE	0	4
12	Rotterdam	ROT	0	7
13	East-Brabant	EBR	0	2
14	Dörpen	DOR	0	1

Figure 4: Case study network representation

In terms of demand for LNG as a fuel, about 500 LNG trucks were operating in the Netherlands in 2017 [Nationaal LNG Platform, 2017]. The goal is to have 5000 LNG trucks in operation in 2020 [SER, 2014b]. In 2017, only 7 ships use LNG as fuel, with plans for another 16 in the near-future. These trucks and ships have fuel tanks with an average capacity of $0.395m^3$ and $45m^3$, and we assume they are refueled three times and once per week, respectively. In line with actual demand, we consider that road demand is evenly spread between all LNG fuel stations, while the demand of ships has a spread of 60% on the larger ports (Amsterdam, Rotterdam, Duisburg) and 40% on the other, smaller ports in the network.

One of the main reasons for the Netherlands being a front runner in the small-scale LNG supply chain development relates to the construction of the GATE terminal in the Port of Rotterdam. Construction of this large-scale import terminal finished in 2011,

and mainly serves the purposes of securing gas supply. Nevertheless, in 2014, GATE terminal expanded its services to enable the uptake of LNG as a fuel. This expansion was completed by the opening of the LNG Break Bulk terminal, where smaller-sized bunker barges can load since 2016. Tanker trucks that can transport LNG from the terminal to the fuel stations and ports are abundantly available, and have a capacity of $50m^3$. In 2017, two bunker barges were under construction. None were yet in use. A bunker barge can be built with various capacities. For the purpose of our study we consider a capacity of $3500m^3$.

5.2 Experimental design

Our experimental design is aimed at gaining insight into the conditions under which one or more satellite terminals will be opened. This decision is driven by economic aspects. Due to specialized resources involved in the small-scale LNG supply chain, the investment in the terminals, bunker barges and tanker trucks in the network translate into important cost elements. Vehicles costs (i.e., for the LNG tanker trucks and bunker barges) consist of initial investment costs, maintenance costs, operational costs, and fuel costs. LNG (satellite) terminals have an initial investment cost and a periodical maintenance cost.

Throughout the experiments, we consider a time horizon of 10 weeks, consisting of 5 periods of 10 working days each. Accordingly, we translated all cost elements into periodic costs. For LNG tanker trucks, the initial investment is around €75,000, which, at a scrap value of 23%, interest rate of 5% and depreciation over 5 years, translates into a cost of €544 per time period. The maintenance costs are €173 (assuming that maintenance costs are 30% of the initial investment) and operational costs are €1,580 per period per truck. Fuel costs are €0.35 per km. Since the capacity of tanker trucks often does not allow for replenishing multiple LNG fuel stations, or visiting multiple ports to service ships, we consider only direct vehicle routes from terminal to a demand point. One tanker truck can make one route per working day, resulting in 10 routes per time period.

The initial investment of an LNG bunker barge is €9,100,000, which, at a scrap value of 20%, interest rate of 5% and depreciation over 30 years, translates into €16,703 per time period. Periodic maintenance costs are €2,692 and operational costs are €1,722. The fuel costs are €9.33 per km. For operational purposes, it is assumed that bunker barges can make 1 route per two days, during which it can serve multiple demand points, but only one satellite.

The initial investment associated with opening a satellite terminal is €1,000,000, which, at a scrap value of 20%, interest rate of 5% and depreciation over 30 years, translates into €2386 per time period. Given the very large investments involved with opening a large-scale LNG terminal (e.g., GATE terminal), and due its much broader purpose than providing LNG as a fuel, not all investment and operational costs translate into costs relevant for the small-scale LNG supply chain. In practice, the specific terminal investments related to facilitating the small-scale LNG supply chain are incurred by means of a fixed fee for bunker barges and tanker trucks when they load the fuel at the terminal. These so-called slot costs are roughly €30,000 for a bunker barge, and €500 for tanker

trucks.

Table 9 represents our experimental design, consisting of four different scenarios changing the slot costs for LNG bunker barges at the import terminal and the investment costs to open, and possibly upgrade, a satellite terminal. It reflects the scenarios where the slot costs are reduced with 50%; upgrading the capacity of the satellite terminal comes at no additional costs; and the entire investment costs associated with a satellite terminal is ignored.

Table 9: Periodic cost parameters for the four scenarios

	Slot cost		Satellite cost	
Scenario	Barge	Truck	Construction	Upgrade
Current costs	€30,000	€500	€2,386	€1,193
50% slot barge	€15,000	€500	€2,386	€1,193
Free upgrades	€30,000	€500	€2,386	€0
50% slot barge + free satellites	€15,000	€500	€0	€0

Each scenario is solved using thirteen different demand instances, as shown in Table 10, representing the real-life demand projections put forward by the industry. For each instance, we consider three different maximum satellite capacity levels, i.e., High (980 m^3), Medium (490 m^3), and Low (210 m^3), where the capacity of a satellite can be upgraded in steps of $70m^3$. This results in 156 unique instances (39 per scenario).

Table 10: Demand instances

Demand instance	# ships	# trucks
1	50	500
2	50	1000
3	50	1500
4	50	2000
5	50	2500
6	50	3000
7	50	3500
8	50	4000
9	50	4500
10	50	5000
11	100	500
12	150	500
13	200	500

5.3 Results

The results of the experiments are depicted in Table 11, where a ✓represents a solution that makes use of a satellite terminal (i.e., where a satellite is opened and used in the vehicle routes).

Table 11: Instances where a satellite is being used in the solution, indicated with ✓

	Instance			Scenarios			
	Demand		Satellite	Current	Free	50% slot	50% slot
	# ships	# trucks	capacity	costs	upgrades	barge	+ free sat
1	50	500	$980m^3$				✓
			$490m^3$				✓
			$210m^3$				
2	50	1000	$980m^3$				✓
			$490m^3$				✓
			$210m^3$				
3	50	1500	$980m^3$				✓
			$490m^3$				✓
			$210m^3$				
4	50	2000	$980m^3$				✓
			$490m^3$				✓
			$210m^3$				
5	50	2500	$980m^3$				✓
			$490m^3$				✓
			$210m^3$				
6	50	3000	$980m^3$				✓
			$490m^3$				✓
			$210m^3$				
7	50	3500	$980m^3$				✓
			$490m^3$				✓
			$210m^3$				
8	50	4000	$980m^3$				✓
			$490m^3$				✓
			$210m^3$				
9	50	4500	$980m^3$		✓	✓	✓
			$490m^3$				✓
			$210m^3$				
10	50	5000	$980m^3$		✓	✓	✓
			$490m^3$				✓
			$210m^3$				
11	100	500	$980m^3$		✓	✓	✓
			$490m^3$				✓
			$210m^3$				
12	150	500	$980m^3$		✓	✓	✓
			$490m^3$				✓
			$210m^3$				
13	200	500	$980m^3$		✓	✓	✓
			$490m^3$				✓
			$210m^3$				

Interestingly, the results indicate that the use of satellite terminals does not provide an economic benefit under current cost levels. Under this scenario, all demand is fulfilled by means of bunker barges and tanker trucks starting and finishing their routes at the large-scale LNG terminal. Hence, the sum of the satellite's construction, upgrade, and maintenance costs is higher than the potential routing cost reduction associated with the vehicles starting from the satellite.

In the scenario where upgrade costs of satellites, which are necessary to increase satellites' initial capacities of $70m^3$, are free, the use of satellites becomes economically beneficial at the largest satellite capacity considered (i.e., $980m^3$) and under high demand (i.e., when either 4500 or 5000 trucks are LNG-fueled, or 100-200 ships sail on LNG). Since, in this Scenario, the additional costs incurred for upgrading the satellite are zero, it is evident that larger satellite capacity is beneficial.

In the scenario where the slot costs of bunker barges decrease by 50%, a similar behaviour in the use of satellites is seen. The use of high capacity satellites provide economic benefits when sufficient LNG demand is present, however, at lower satellite capacities, no satellites are opened. The rational behind the need for larger satellite capacity is that it allows supply in large, cost-effective, quantities to the satellite.

Finally, we considered the situation where satellites would be completely free. Although this is obviously not a realistic setting, we considered it to see if, from a routing perspective it would make sense to open satellite. In this scenario (i.e., where the slot costs are decreased with 50% and satellite construction and upgrade costs are zero), satellites are opened in all demand instances, but only at Medium (i.e., $490m^3$) or High (i.e., $980m^3$) satellite capacity. Interestingly, the use of low capacity satellites is not beneficial, even when their construction is free. The reason is that, albeit relatively low, the slot cost of the bunker barge at the large-scale terminal is weighing heavily on the operational costs of the network, which can only be compensated by large quantity supplies to a satellite.

Overall, our results indicate that investments in satellite terminals should be considered with care. Both the slot costs at the large-scale LNG terminal, which are incurred when supplying the satellite, and the construction/upgrade costs of the satellite lead to a large operational cost component, which is not easily compensated by a reduction in routing costs. We note that we studied the European small-scale LNG infrastructure, and in particular the rollout of that infrastructure from the Netherlands. As a result, the large-scale LNG terminal is relatively nearby, which has an effect on the routing cost reductions that can be gained from opening a satellite. A reduction of the slot costs or lower satellite construction costs considered in our experiments have a similar effect on the network design.

6 Conclusions

Inspired by a real-life network design problem related to the expansion of the European small-scale LNG supply chain, this paper proposes the complex Two-Echelon Location Routing Problem with Split Deliveries. Allowing direct shipments from terminals at

different levels of the supply chain to the end-consumers makes this location routing problem much more complex to solve. We have significantly improved the performance of a hybrid exact algorithm, which clearly outperforms its previous version and also the solution of a state-of-the-art commercial solver. Smaller and less complex instances were solved optimally using 44.8% less computation time on average. The relative performance gap for larger and more complex instances decreased with 14.93% on average. A detailed case study sheds light on the development, operations, and economic performance of opening satellite terminals when expanding the Dutch small-scale LNG supply chain into Europe.

References

Z Akca, RT Berger, and T Ralphs. Modeling and solving location routing and scheduling problems. In *Proceedings of the eleventh INFORMS computing society meeting*, pages 309–330, 2008.

M. Albareda-Sambola, J. A. Diaz, and E. Fernández. A compact model and tight bounds for a combined location-routing problem. *Computers & Operations Research*, 32(3): 407–428, 2005.

M. Albareda-Sambola, E. Fernández, and S. Nickel. Multiperiod location-routing with decoupled time scales. *European Journal of Operational Research*, 217(2):248–258, 2012.

A. Balakrishnan, J.E. Ward, and R.T. Wong. Integrated facility location and vehicle routing models: Recent work and future prospects. *American Journal of Mathematical and Management Sciences*, 7(1-2):35–61, 1987.

Roberto Baldacci, Aristide Mingozzi, and Roberto Wolfler Calvo. An exact method for the capacitated location-routing problem. *Operations Research*, 59(5):1284–1296, 2011.

Sérgio dos Santos Barreto. Análise e modelização de problemas de localização-distribuição. *tese de doutoramento, Gestao Indústrial, Universidade de Aveiro, Aveiro, Portugal*, 2004.

E. Boventer. The relationship between transportation costs and location rent in transportation problems. *Journal of Regional Science*, 3(2):27–40, 1961.

C. Contardo, J.-F. Cordeau, and B. Gendron. An exact algorithm based on cut-and-column generation for the capacitated location-routing problem. *INFORMS Journal on Computing*, 26(1):88–102, 2013.

R. Cuda, G. Guastaroba, and M. G. Speranza. A survey on two-echelon routing problems. *Computers & Operations Research*, 55:185–199, 2015.

M. Drexl and M. Schneider. A survey of variants and extensions of the location-routing problem. *European Journal of Operational Research*, 241(2):283–308, 2015.

A. Duarte, N. Mladenović, J. Sánchez-Oro, and R. Todosijević. Variable neighborhood descent. In R. Martí, P. Panos, and M. G.C. Resende, editors, *Handbook of Heuristics*, pages 1–27. Springer International Publishing, Cham, 2016.

J. W. Escobar, R. Linfati, M.G. Baldoquin, and P. Toth. A granular variable tabu neighborhood search for the capacitated location-routing problem. *Transportation Research Part B: Methodological*, 67:344–356, 2014.

G. Guastaroba, M. G. Speranza, and D. Vigo. Intermediate facilities in freight transportation planning: a survey. *Transportation Science*, 50(3):763–789, 2016.

J. Hof, M. Schneider, and D. Goeke. Solving the battery swap station location-routing problem with capacitated electric vehicles using an avns algorithm for vehicle-routing problems with intermediate stops. *Transportation Research Part B: Methodological*, 97: 102–112, 2017.

I. Karaoglan, F. Altiparmak, I. Kara, and B. Dengiz. The location-routing problem with simultaneous pickup and delivery: Formulations and a heuristic approach. *Omega*, 40 (4):465–477, 2012.

GJ Kasper. Transportbrandstof uit biogas geeft hoger rendement en verduurzaamt. *V-focus*, 10(6):24–26, 2013.

Ç. Koç, T. Bektaş, O. Jabali, and G. Laporte. The impact of depot location, fleet composition and routing on emissions in city logistics. *Transportation Research Part B: Methodological*, 84:81–102, 2016.

R. Lahyani, L. C. Coelho, and J. Renaud. Alternative formulations and improved bounds for the multi-depot fleet size and mix vehicle routing problem. *OR Spectrum*, 40(1): 125–157, 2018.

G. Laporte, Y. Nobert, and S. Taillefer. Solving a family of multi-depot vehicle routing and location-routing problems. *Transportation Science*, 22(3):161–172, 1988.

H. Larrain, L. C. Coelho, and A. Cataldo. A variable mip neighborhood descent algorithm for managing inventory and distribution of cash in automated teller machines. *Computers & Operations Research*, 85:22–31, 2017.

F. E. Maranzana. On the location of supply points to minimize transport costs. *Journal of the Operational Research Society*, 15(3):261–270, 1964.

M.B.C. Menezes, D. Ruiz-Hernández, and V. Verter. A rough-cut approach for evaluating location-routing decisions via approximation algorithms. *Transportation Research Part B: Methodological*, 87:89–106, 2016.

H. Min, V. Jayaraman, and R. Srivastava. Combined location-routing problems: A synthesis and future research directions. *European Journal of Operational Research*, 108 (1):1–15, 1998.

N. Mladenović and P. Hansen. Variable neighborhood search. *Computers & Operations Research*, 24(11):1097–1100, 1997.

G. Nagy and S. Salhi. Location-routing: Issues, models and methods. *European Journal of Operational Research*, 177(2):649–672, 2007.

Nationaal LNG Platform. Waar kunnen trucks nu en binnenkort LNG tanken?, 2017. URL `http://www.nationaallngplatform.nl/waar-kunnen-trucks-lng-tanken/`.

Jossef Perl and Mark S Daskin. A warehouse location-routing problem. *Transportation Research Part B: Methodological*, 19(5):381–396, 1985.

Roel Post, Paul Buijs, Michiel uit het Broek, Jose Lopez Alvarez, Nick Szirbik, and Iris Vis. A solution approach for deriving alternative fuel station infrastructure requirements. *Flexible Services and Manufacturing Journal*, pages 1–16, 2017.

C. Prins, C. Prodhon, A. Ruiz, P. Soriano, Wolfler, and R. Calvo. Solving the capacitated location-routing problem by a cooperative lagrangean relaxation-granular tabu search heuristic. *Transportation Science*, 41(4):470–483, 2007.

Christian Prins, Caroline Prodhon, Wolfler, and Roberto Calvo. Solving the capacitated location-routing problem by a grasp complemented by a learning process and a path relinking. *4OR*, 4(3):221–238, 2006.

C. Prodhon. A hybrid evolutionary algorithm for the periodic location-routing problem. *European Journal of Operational Research*, 210(2):204–212, 2011.

C. Prodhon and C. Prins. A survey of recent research on location-routing problems. *European Journal of Operational Research*, 238(1):1–17, 2014.

J. Rieck, C. Ehrenberg, and J. Zimmermann. Many-to-many location-routing with inter-hub transport and multi-commodity pickup-and-delivery. *European Journal of Operational Research*, 236(3):863–878, 2014.

F.A. Santos, G.R. Mateus, and A.S da Cunha. A branch-and-cut-and-price algorithm for the two-echelon capacitated vehicle routing problem. *Transportation Science*, 49(2): 355–368, 2015.

M. Schneider and M. Löffler. Large composite neighborhoods for the capacitated location-routing problem. *Transportation Science*, forthcoming, 2017.

SER. A vision on sustainable fuels for transport. *Technical Report*, 2014a.

SER. Brandstoftafel wegvervoer duurzaam gasvormig. *Deelrapport*, 2014b.

Simon Thunnissen, Luke van de Bunt, and Iris Vis. Sustainable fuels for the transport and maritime sector: A blueprint of the LNG distribution network. In *Logistics and Supply Chain Innovation*, pages 85–103. Springer, 2016.

Dilek Tuzun and Laura I Burke. A two-phase tabu search approach to the location routing problem. *European Journal of Operational Research*, 116(1):87–99, 1999.

R Verbeek and M Verbeek. LNG for trucks and ships: fact analysis review of pollutant and ghg emissions. *TNO report*, page 70, 2015.

C. D. T. Watson-Gandy and P. J. Dohrn. Depot location with van salesmen – a practical approach. *Omega*, 1(3):321–329, 1973.

Hengbing Zhao, Andrew Burke, and Lin Zhu. Analysis of class 8 hybrid-electric truck technologies using diesel, LNG, electricity, and hydrogen, as the fuel for various applications. In *Electric Vehicle Symposium and Exhibition (EVS27), 2013 World*, pages 1–16. IEEE, 2013.